# Negative Poisson ratio in poly(tetrafluoroethylene) monitored spectroscopically

**Bret W. Ludwig and Marek W. Urban***
*Department of Polymers and Coatings, North Dakota State University, Fargo, ND 58105, USA*
*(Received 9 December 1992; revised 10 June 1993)*

Morphological changes resulting from the elongation of poly(tetrafluoroethylene) (PTFE) have been examined using rheo-photoacoustic Fourier transform infra-red (r.p.a. *FT*i.r.) methodology. Based on the quantitative analysis of the r.p.a. *FT*i.r. data, several transitions in the film permeability are identified over the range of examined elongations, and the mechanism responsible for these transitions is discussed. Electron microscopy and X-ray diffraction measurements were utilized in an attempt to further support the proposed mechanism of elongation in the negative Poisson ratio region. In contrast to polyethylene and other polymers, this phenomenon is characteristic of PTFE. The strain dichroic ratios obtained using transmission *FT*i.r. spectroscopy are not sensitive to these transitions.

**(Keywords: poly(tetrafluoroethylene); negative Poisson ratio; spectroscopy)**

## INTRODUCTION

Among the many factors affecting transport properties and diffusion rates of small molecules in polymeric materials, the polymer morphology is one of the primary contestants[1-7]. For this reason, the rates at which diffusants migrate through a polymer network wll provide further insights into polymer microscopic structure[5-7]. Our recent studies showed that morphological changes are indeed responsible for many properties that occur as a result of polymer elongation, and may strongly influence the diffusion rate[7].

This issue is particularly important in polymer networks having crystalline and amorphous components, because it is commonly known that the uniaxial elongation of randomly oriented amorphous chains and crystalline components results in orientation of crystallites parallel to the strain axis. Another aspect is that polymers experience more oriented morphologies as a result of elongation and may exhibit either diminished or enhanced rates of diffusion[8,9]. As the ordering increases with elongation, it may allow a closer spatial packing of chains and crystallites. This will reduce the number of diffusion pathways and, consequently, slow down the diffusion processes. In the case of semicrystalline polymers, it is more common for the diffusion rates to increase upon elongation. This results from an increase of free volume in the amorphous phase, which is a consequence of the presence of a crystalline phase. The latter may interfere with the lateral contraction of the polymer film[1]. The amorphous-phase chains become oriented parallel to one another, but the non-deformable crystals prevent close packing. In this case the volume of the amorphous phase increases and the density decreases, resulting in higher diffusion rates. This effect, however, may not be the case for all semicrystalline polymers that experience uniaxial elongation. While many polymers, in addition to the above phenomena, may experience phase transitions inducing new crystalline phases, poly(tetrafluoroethylene) (PTFE), when elongated, demonstrates the rather unusual phenomenon of thickening in the direction perpendicular to the strain axis. This effect is referred to as a negative Poisson ratio (*NPR*) and it has been found that prerolled PTFE has an *NPR* up to 17% strain[10,11] This behaviour has been attributed to a rotation of anisotropic crystals within the film.

In this study, we address the origin of the structural changes that occur in PTFE upon elongation in the *NPR* region. For this purpose, we utilize rheo-photoacoustic Fourier transform infra-red (r.p.a. *FT*i.r.) spectroscopy to monitor polymer permeability[12] and non-equilibria in polymers[13], along with X-ray diffraction measurements to follow changes in crystal orientation resulting from elongation, and scanning electron microscopy for visual assessment of the film thickness changes upon elongation.

## EXPERIMENTAL

PTFE films ($125 \pm 5\ \mu m$ thick) were obtained from PTFE Industries. Perfluoro(methylcyclohexane) (PFMCH) was purchased from Aldrich Chemical and was used without further purification. Dumbbell shaped samples with a length of 75 mm, end width of 13 mm, notch length of 25 mm and notch width of 7 mm were placed in PFMCH for a minimum of 4 days to allow complete saturation.

Relative diffusion rates of PFMCH were determined using an r.p.a. *FT*i.r. technique recently developed in our laboratory[7,13]. The technique relies on finding a volatile solvent which will swell a polymer film. In the case of PTFE, PFMCH was found to be the most

* To whom correspondence should be addressed

0032-3861/94/23/5130-08

suitable solvent[14], swelling the film sufficiently to allow determination of the diffusion rate by monitoring its desorption.

Following saturation PTFE samples were loaded into an r.p.a. cell[15–17], and strained to 0–50%. R.p.a. *FT*i.r. spectra were obtained by co-adding 400 scans collected with a resolution of 4 $cm^{-1}$ using a Digilab FTS-10 i.r. spectrometer. As described elsewhere[7], the experimental set-up was such that the incident i.r. light interacted only with the PFMCH vapour. This was achieved by using aluminium foil as a 'photoacoustic umbrella'[13], intercepting the i.r. light before it impinged on the film surface. The spectra were collected continuously, allowing for an initial 2 min purge of the r.p.a. cell with He before collection of the first spectrum, and 30 s purges between successive spectra. In addition to the experiments performed on films saturated with PFMCH, a second set of experiments was performed on samples that were exposed to ambient conditions for 30 min prior to the experiment. This resulted in a reduced concentration of PFMCH in the PTFE when the monitoring of the diffusion rate was begun. All other experimental conditions remained unchanged.

X-ray diffractograms were acquired on a Phillips diffractometer operated at 45 kV and 30 mA, using a long Cu fine focus tube. Diffractograms were collected between 16 and 45° $2\theta$, with a resolution of 0.03125° $2\theta$, and at intervals of 1 s. The PTFE samples were strained at a rate of 1% $s^{-1}$ and held at a constant strain by an aluminium clamp designed for use in the diffractometer. Scanning electron micrographs of the film cross-sections upon various elongations were obtained on a Jeol 310 scanning electron microscope at a magnification of 500, applying 10 kV accelerating voltage. A Polaroid camera attached to the scanner was used to obtain photographs.

The degree of crystallinity of the PTFE films under investigation was determined gravimetrically. Values of 2.0 and 2.285 g $cm^{-3}$ were used for the densities of the amorphous and crystalline phases, respectively[18]. A value of 55% was determined for the weight fraction of crystalline material within our sample.

## RESULTS AND DISCUSSION

The r.p.a. *FT*i.r. gas-phase spectrum of PFMCH is shown in *Figure 1*. The integrated intensity of the 976 $cm^{-1}$ band, attributed to a C–F deformation of the fluorine group attached to a cyclohexane ring[19], will be used to determine the rate at which PFMCH diffuses through PTFE. However, in order to evaluate the data in terms of the rate of diffusion of the solvent within the film, the relationship between the r.p.a. intensity and the rate of diffusion should be established. If one assumes that the intensity of each subsequent r.p.a. spectrum is proportional to the amount of solvent entering the vapour phase during the time the spectrum was collected, then the amount of solvent evaporating from the film is proportional to the amount of solvent being able to reach the surface. This, in turn, depends on the rate of diffusion within the film[20], following the initial stages of evaporation. As a result, the intensity of the r.p.a. signal during the time the spectrum was collected can be taken to be proportional to the diffusion coefficient of the solvent near the film surface.

Before we attempt to establish the relationship between r.p.a. intensity and time during which diffusion occurs,

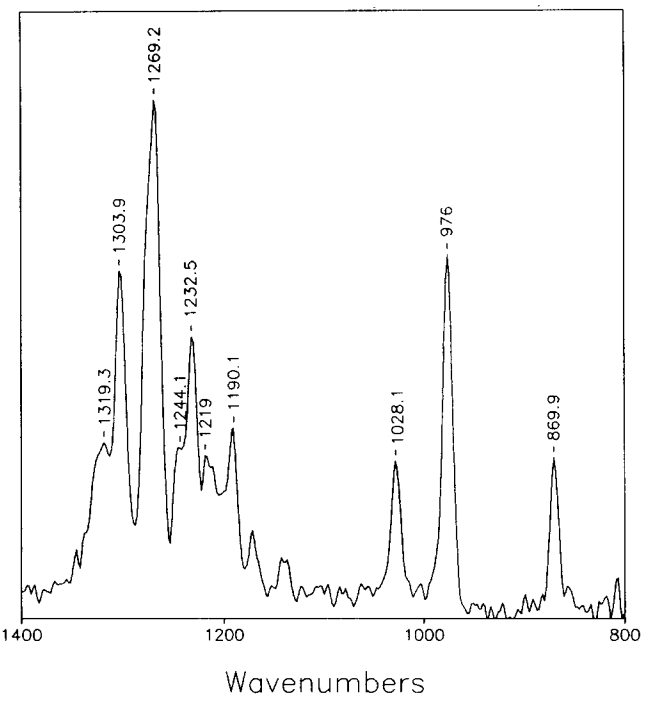


**Figure 1** R.p.a. *FT*i.r. spectrum of perfluoro(methylcyclohexane) vapour

it should be realized that the relationship between concentration of diffusant molecules and the diffusion coefficient is given by[21]:

$$D = D_0 e^{kC/C_0} \quad (1)$$

where $D$ is the diffusion coefficient at concentration $C$, $D_0$ is the diffusion coefficient at concentration of diffusant $C_0$ in a saturated film, and $k$ is a system dependent constant. The relationship between the fractional loss ($C/C_0$) and the square root of time yields a curve concave to the time axis.

With this in mind, let us now establish the relationship between r.p.a. intensity and time, which is given by:

$$I = A\exp(-xt^{1/2}) \quad (2)$$

where $I$ is the integrated intensity of the band, $A$ is a pre-exponential factor, $x$ is the rate at which diffusant molecules diffuse out of the polymer, and $t$ is the time measured from the removal of the film from the PFMCH solution. Equation (2) is analogous to equation (1) because the r.p.a. intensity is proportional to the rate of diffusion during the spectral collection. As a result, $I$ in equation (2) will be equivalent to $D$ in equation (1). Similar analogies can be drawn for $A$ and $D_0$. As a matter of fact, Crank[21] demonstrated the relationship between concentration and $t^{1/2}$ for a concentration-dependent diffusion coefficient, and by taking the slope of ln $I$ with respect to $t^{1/2}$ as a measure of diffusion, one obtains a value that is proportional to the rate of change of $D$ over time. Thus, using $x$ as a measure of the rate of diffusion provides a means of determining the relative diffusion rates for various polymer morphologies.

Similarly to the procedures developed for poly(vinylidene fluoride)[22], a plot of the 976 $cm^{-1}$ band area *versus* time, measured from the removal of the sample from PFMCH, at which the first 200 scans of the 400 co-added scan spectrum were collected, results in a curve that fits equation (1)[22]. A plot of the natural log of the intensity of the band *versus* the square root of time yields a straight

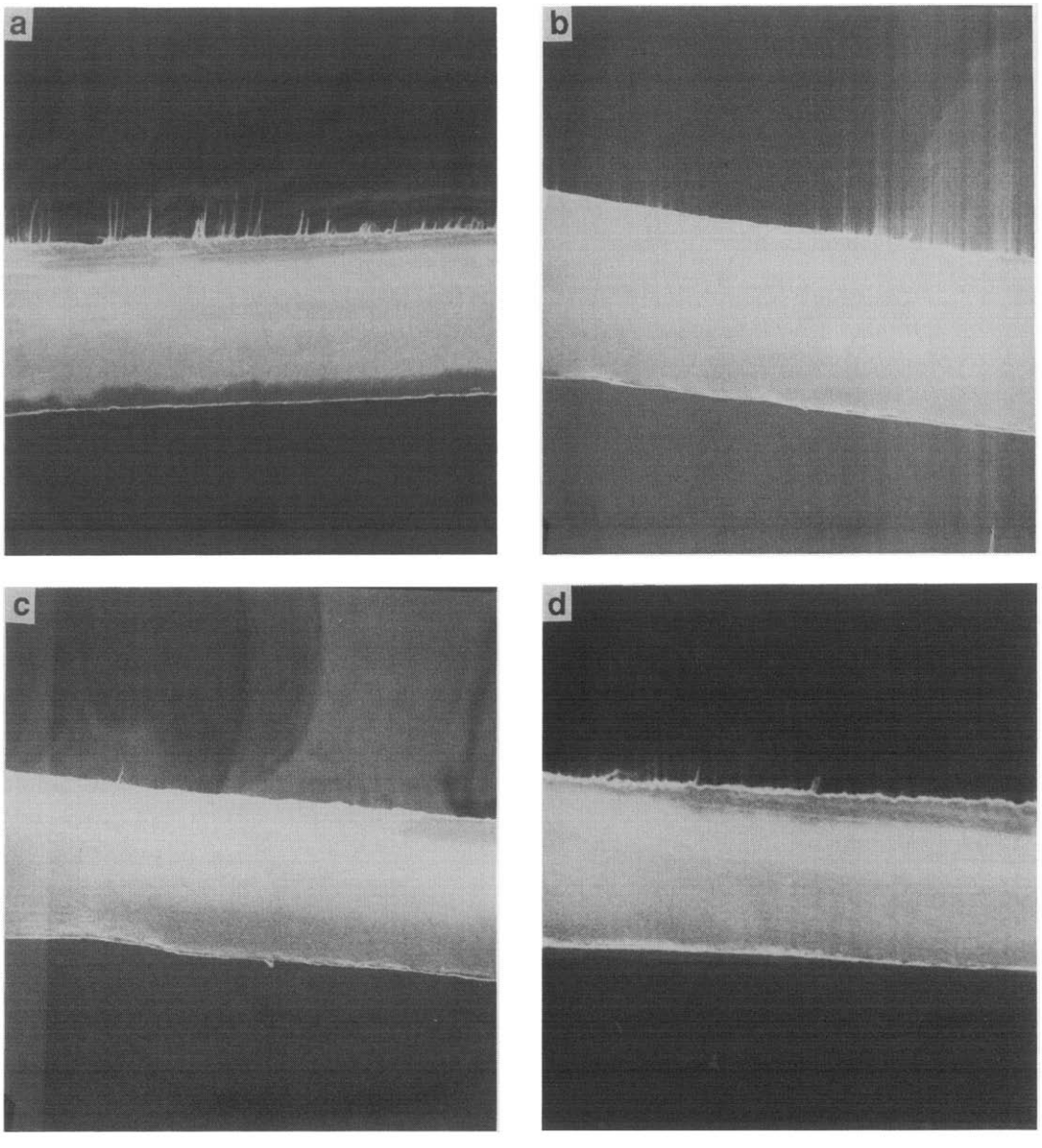


**Figure 2** Electron micrographs of PTFE film edge: the films were strained to (a) 0%; (b) 5%; (c) 10%; and (d) 20% elongation

line with slope $x$. The faster the solvent diffuses to the surface and evaporates from the film and is subsequently purged away between spectra, the larger the value of $x$.

In an effort to determine the effect of an *NPR* on the permeability of PTFE, a few issues should be addressed. First of all, it should be realized that the morphology of this polymer is significantly different from that previously reported to demonstrate an *NPR*. Thus, when undertaking a comparison of our results with those reported in the literature[10,11], and subsequently the structures proposed to account for the reported results, it is important to remember that the films studied by Evans and Caddock[10,11] were prerolled prior to elongation. The purpose of such a sample modification was to maximize the initial orientation of the disc-like crystals parallel to the plane of the film. In our case, we will use as-received PTFE and, in an effort to prove that our unmodified material demonstrates the *NPR* effect, electron microscopy was used. *Figures 2a–d* show electron micrographs of the cross-section of a 125 $\mu$m thick PTFE film at 0, 5, 10 and 20% elongations, respectively. The expansion of the film perpendicular to the strain axis is apparent at 5 and 10% strains, demonstrating that our unmodified samples also expand upon elongation.

A considerable amount of evidence exists that for PTFE, an *NPR* occurs at low strains[10,11], and is primarily related to the rotations of crystals perpendicular to the strain axis. If the proposed model is indeed valid, let us predict what one may expect when monitoring the diffusion rate as a function of strain. An initial, moderate increase of the diffusion coefficient ($D$), due to an increase in the free volume of the amorphous phase, would be expected, and a further decrease of the amorphous phase density should occur upon rotation of the anisotropic crystals, resulting in increases of free volume and $D$. Upon further straining, the film is expected to become porous as it is transformed to a fibrous morphology. The porous structure would provide open transport paths to the surface, which may further increase $D$. With this in mind, straining PTFE is expected to result in a continuous increase of $D$, with a transition in the rate of increase of $D$ indicating the onset of crystalline rotation, and possibly a second transition due to the onset of void formation.

Before we approach the analysis of an *NPR*, it is first

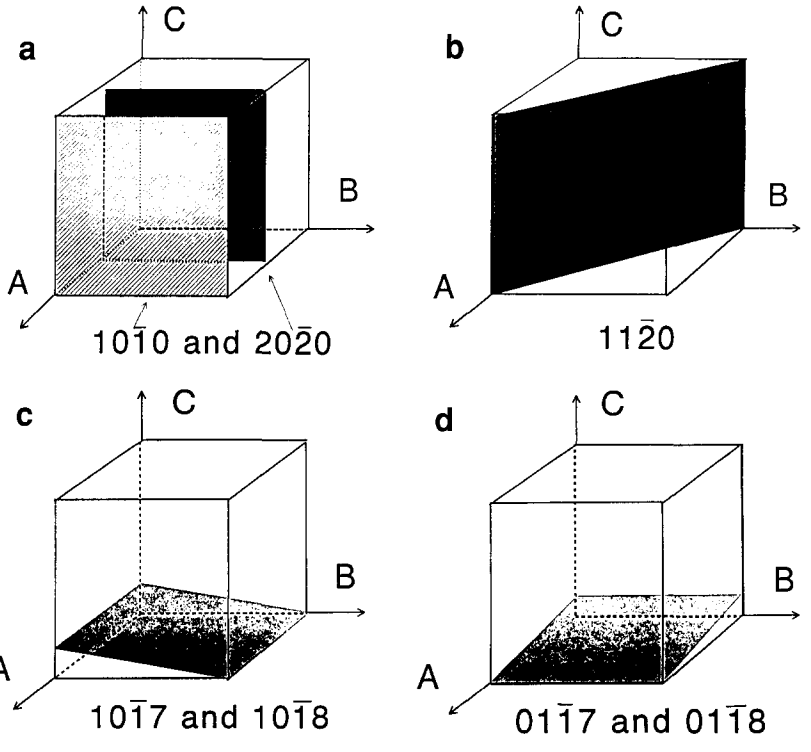


**Figure 3** Crystalline planes in PTFE: (a) 1010 and 2020 planes; (b) 1120 plane; (c) 1017 and 1018 planes; (d) 0117 and 0118 planes

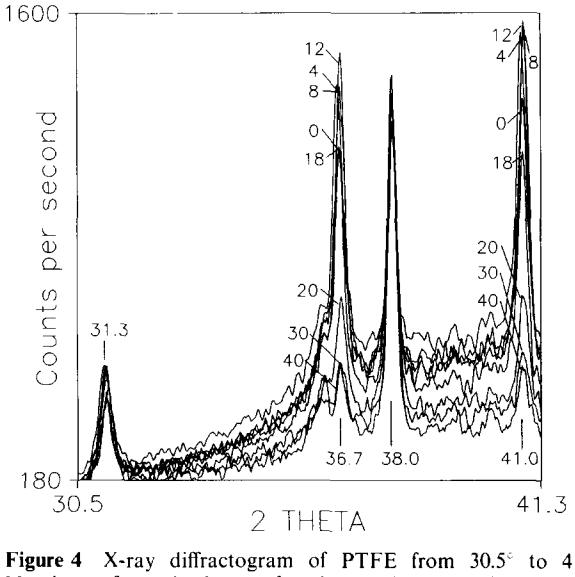


**Figure 4** X-ray diffractogram of PTFE from 30.5° to 41.5° 2θ. Numbers refer to the degree of strain experienced by the specimen from which the diffractograms were recorded

necessary to interpret the information obtained from X-ray analysis, and to correlate the peak assignments with the crystallographic planes responsible for the reflections. A simplified representation of the relevant PTFE crystalline planes is shown in *Figure 3*. The polymer chain axis is assumed to be parallel to the c axis. *Figure 3a* shows the 1010 and 2020 planes which are responsible for reflections at 17.7° and 36.4° 2θ, respectively[22]. *Figure 3b* depicts the 1120 plane which accounts for the reflection at 31.3° 2θ, whereas *Figures 3c* and *d* represent the 1017 and 0117 planes, responsible for the reflection at 36.7° 2θ, and the 1018 and the 0118 planes, which contribute the 41.0° 2θ peak to the diffractogram.

A preliminary examination of the planes' orientation relative to the crystal axis reveals that the crystals with c axis parallel to the plane of the film will indeed contribute to the intensity of diffractogram peaks at 17.7°, 31.3° and 36.4° 2θ. Crystals whose c axis is perpendicular to the plane would account for peaks at 36.7° and 41.0° 2θ. *Figure 4* presents the diffractograms between 30.5° and 41.5° 2θ of PTFE strained to 0–40%. In addition to the peaks at 36.7° and 41.0° 2θ, a third peak is apparent in the diffractogram at 38° 2θ. This peak is due to the aluminium clamp used to hold the samples at constant strain. Diffractograms of the corresponding 17.1° to 18.1° 2θ region are shown in *Figures 5a* and *b*.

At this point let us return to our main theme and use the diffusion and X-ray diffraction results to analyse the structural changes that occur in PTFE as a function of strain. Utilizing the X-ray diffraction results, we shall discuss each transition in the rate of diffusion separately, in an effort to aid in the interpretation of the structural changes. Curves A and B of *Figure 6a* represent the results of the diffusion rate experiments outlined in the Experimental section. Curve C in *Figure 6b* represents the integrated intensity of the peak at 17.7° 2θ seen in *Figure 5*. When examining the data presented in *Figure 6*, it must be remembered that each data point for the rate of diffusion is obtained by monitoring the desorption of PFMCH as a function of time. All experiments were conducted in the same time frame, so the rates of diffusion reported at each strain are obtained from films saturated with PFMCH (curve A), or dried for precisely 30 min prior to elongation (curve B).

In order to clarify the existence of the two minima in the diffusion rate and eliminate any concerns over the influence of the rapidly changing concentration of diffusant in the early stages of evaporation, the data in curve B of *Figure 6a*, were collected. Following 30 min of evaporation, the rate of diffusion is considerably

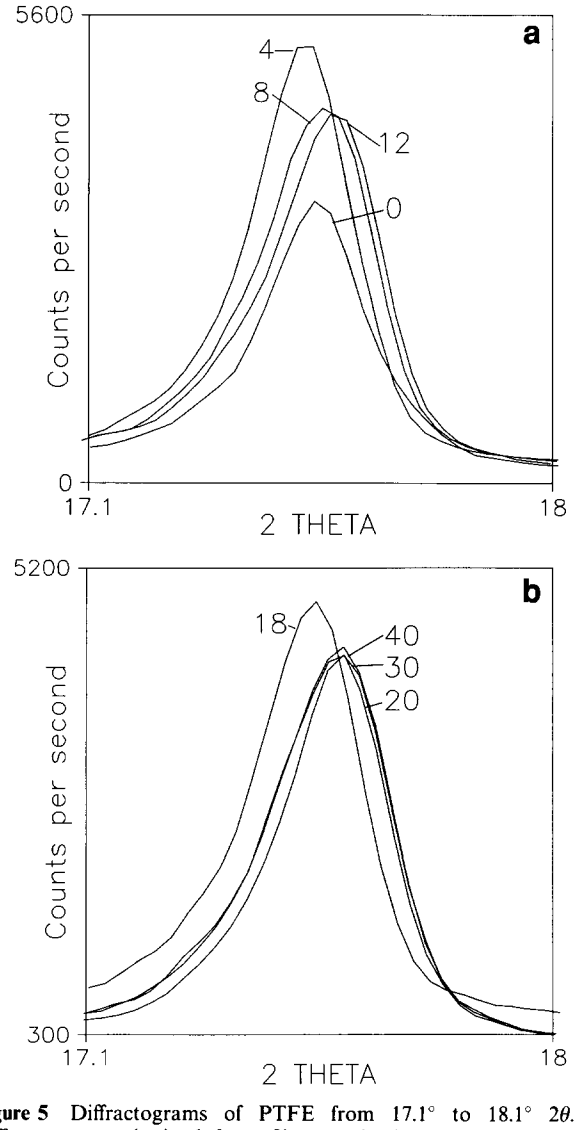


**Figure 5** Diffractograms of PTFE from 17.1° to 18.1° $2\theta$. (a) Diffractograms obtained from films strained to 0, 4, 8 and 12% elongation; (b) diffractograms obtained from films strained to 18, 20, 30 and 40% elongation

reduced, as evidenced by the smaller values of $x$ obtained from equation (1). This is due to the concentration dependence of $D$[3,23,24]. As can be seen in *Figures 6a* and *b*, the transitions in the rate of diffusion appear at the same elongations for both the saturated and the non-saturated films. Kinetic effects due to the decreasing concentration of PFMCH in the film as a function of time are therefore eliminated from consideration as an explanation for the variable rate of diffusion as a function of strain. The variation of the diffusion rate is therefore attributed to structural changes occurring upon elongation.

As indicated in *Figure 6a*, the initial rapid decrease of the diffusion rate up to 4% strain is somewhat surprising. This behaviour may be attributed to intercrystalline amorphous-phase chains being pulled taut, limiting the mobility of other amorphous-phase chains and thereby causing a decrease of the PTFE free volume. As determined gravimetrically, the crystallinity of the PTFE specimens used in this study was on the order of 55%. The tie molecules in such a highly crystalline film may be of relatively short length and upon imposed stresses, they can be quickly pulled taut, thus limiting diffusion. However, another possibility is that the decrease of the diffusion rate with increasing strain is due to a reorganization of the polymer morphology such that more crystals are oriented parallel to the plane of the film. As more impermeable crystals align parallel to the plane of the film, diffusants must take longer paths around them in order to reach the film surface. As shown in *Figure 5a*, the intensity of the peak at 17.7° $2\theta$ increases when going from 0 to 4% strain, indicating an increase in the number of crystallites lying horizontal to the film plane. Incidently, the 17.7° $2\theta$ peak intensity changes illustrated in *Figure 6b* follow almost exactly the same trend detected for the diffusion data in *Figure 6a*. An increased intensity of the 36.7° and 41.0° $2\theta$ peaks also appears at 4% strain (*Figure 4*), indicating that the orientation of those crystals that were nearly perpendicular to the draw direction is beginning to undergo rearrangement. For such a large restructuring of the crystallites within the film, stress must be efficiently transferred to the crystallites, requiring the tightening of the intercrystalline tie molecules. Thus, it appears that an increased order in the amorphous regions, as well as an enhanced tortuosity of the diffusion path due to the alignment of crystallites, account for the slowed diffusion rates during the first stage of deformation.

Further analysis of the results presented in *Figures 6a* and *b* indicates that between 4 and 12% strain, a rapid increase in the diffusion rate is observed. This observation corresponds well with the decrease of the 17.7° $2\theta$ peak and the electron micrograph shown in *Figure 2b*. This increase in the rate of diffusion can be attributed to the restructuring of the polymer film's morphology as more tie molecules are pulled taut. As the degree of strain increases, those crystallites that were oriented perpendicular to the strain axis will rotate parallel to the axis. If no crystals are concurrently rotating into a perpendicular alignment, the intensity of the peaks at 36.7° and 41.0° $2\theta$ would be expected to decrease, because crystal planes responsible for these peaks are no longer in the proper orientation to contribute to the diffraction intensity. However, there is no change in the intensity of these peaks between 4 and 12% strain, as seen in *Figure 4*, indicating that there is no net change in the number of crystals oriented perpendicular to the draw direction during the straining of the film from 4 to 12% strain. This suggests that a significant fraction of crystals, not aligned parallel to the film surface, rotate perpendicular to the film surface as they move to assume an orientation parallel to the draw direction. The disruption that these rotating crystals introduce to the film is demonstrated in *Figure 5a* by a decrease of the 17.7° $2\theta$ peak, which signifies that a portion of the crystals that were parallel to the draw direction are displaced from their parallel alignments. A less favourable explanation for the decrease of this peak is that the tie molecules interact with the crystallites in such a way as to cause some crystals with an essentially parallel alignment to rotate out of alignment. The rotation of the crystals perpendicular to the draw direction will increase the thickness of the film, resulting in an *NPR*, as seen in the micrographs in *Figure 2*. The decreased order of the crystalline phase during this transition decreases the tortuosity of the diffusion paths through the film. This, in combination with a significant decrease in the amorphous phase density caused by the large volume

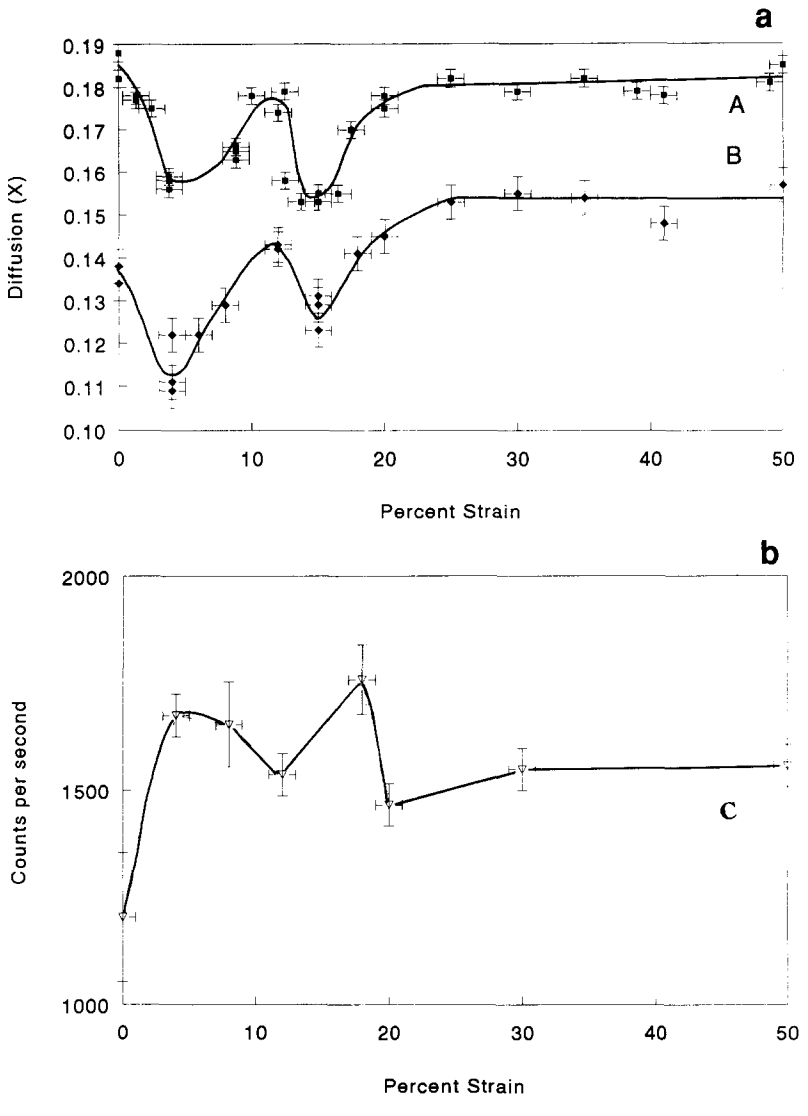


**Figure 6** (a) Relative diffusion rates recorded using r.p.a. *FTi.r.* plotted in terms of $x$ values obtained from equation (1): A, saturated PTFE; B, nonsaturated PTFE exposed for 30 min before measurements. (b) Integrated intensity of the 17.7° $2\theta$ peak

increase during the *NPR* transition, increases the rate of diffusion.

A third transition in the diffusion and X-ray diffraction data is evident between 12 and 17% strain, as illustrated in *Figures 6a* and *b*. The permeability decreases rapidly during this stage of deformation. This observation correlates well with the contraction of the film, which appears to occur between 10 and 20% elongation, as illustrated by the micrographs in *Figures 2c* and *d*. The corresponding increase of the 17.7° $2\theta$ intensity is also seen in *Figure 5*, indicating a greater number of crystals oriented parallel to the plane of the film. Furthermore, the large drop of the 36.7° and 40.0° $2\theta$ peaks over the same range of elongations, shown in *Figure 4*, indicates that fewer crystals are oriented perpendicular to the draw direction. As a large fraction of the crystals oriented perpendicular to the draw direction are brought into parallel alignment, the overall order in the film is greatly enhanced. With more crystals now oriented parallel to the draw direction, the diffusion paths are more tortuous, and with a significant fraction of the crystalline rotations completed, there are fewer disruptions of the amorphous phase. As a result, an overall increase of the density occurs. The increased density, which corresponds to a decreased free volume, in addition to the greater overall orientation of the crystalline phase results in the decreased diffusion rate observed at approximately 17% strain.

At this point, let us consider the ways that polymer networks may respond to external stresses. The polymeric chains of a non-oriented film will most likely assume an orientation parallel to the applied load in order to relieve stresses. On the other hand, polymer films with a high degree of order do not have too many choices, and the application of stresses will most likely induce either slippage of polymer chains and crystals past one another or chain rupture. In the case of PTFE, when the degree of strain reaches 17%, there are regions within the polymer which have attained such a high degree of alignment that slippage and chain rupture are the only means of stress relaxation available. These mechanisms result in the formation of microvoids within the film and a decrease in the overall order, as illustrated by the decrease in the intensity of the diffraction peak at 17.7° $2\theta$ in *Figure 5b*. It is this microvoid formation that provides unhindered pathways through the film, greatly enhancing the rate of diffusion. The overall order of the film increases between 20 and 40% strain. This is demonstrated in *Figure 4* by the near disappearance of the 36.7° and 40.0° $2\theta$ peaks, and the dramatic decrease

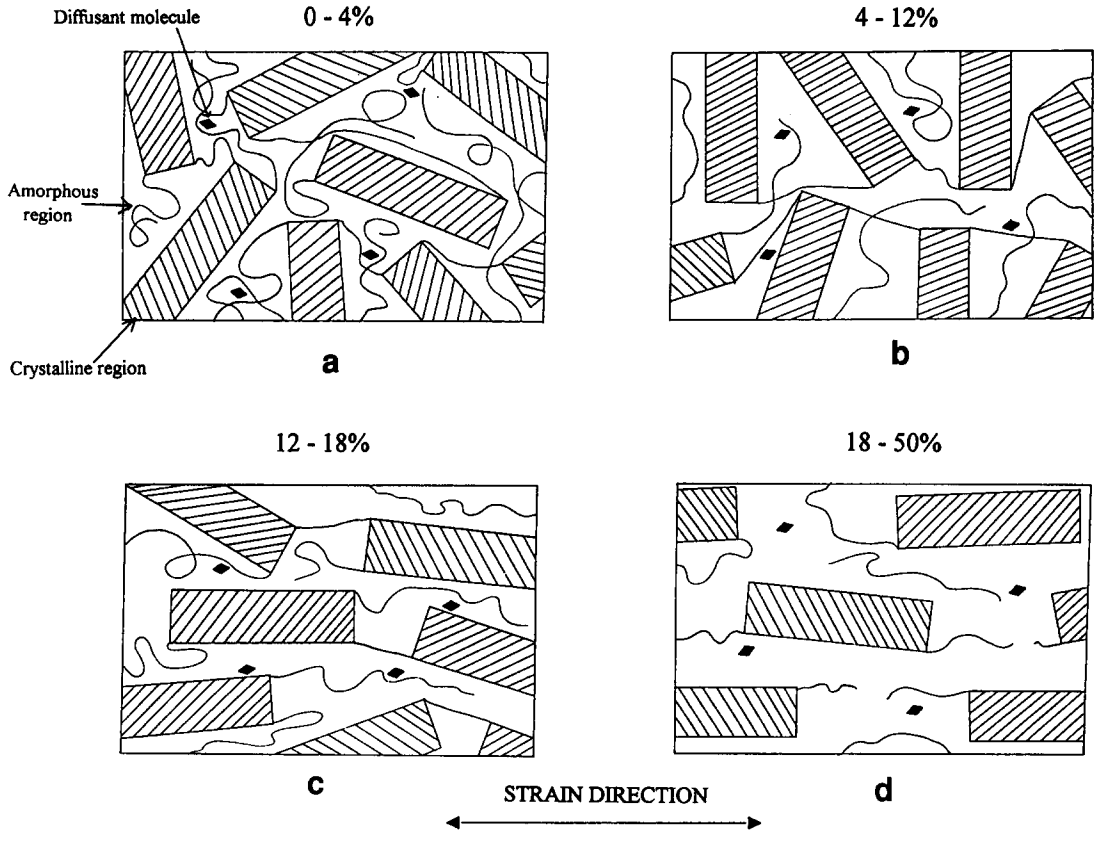


**Figure 7** Morphological changes in PTFE as a function of elongation. (a) 0 to 4% strain — crystallites have random orientation, a fraction of the tie molecules are pulled taut, and reduced permeability is observed; (b) 4 to 12% strain — tie molecules induce rotation of crystallites perpendicular to the film plane and, as a result, amorphous phase density decreases and enhanced permeaility is observed; (c) 12 to 18% strain — further rotation of crystallites results in parallel orientation of crystallites to the film plane, slowing diffusion; (d) 18 to 50% strain — as a result of crystallite slippage and chain rupture, microvoids are formed and permeability increases

of the amorphous halo, which indicates a significant ordering of the amorphous regions. The increase in ordering is also demonstrated by a small increase in the intensity of the 17.7° $2\theta$ peak. Beyond 20% strain, despite the increase in order, the permeability of the film remains approximately constant because PTFE takes on a fibrous structure which does not change the permeability of the voids. Once microvoids have formed within the polymer, further morphological changes will have marginal effect on permeability.

A comparison of the diffusion rates at 0 and 50% strains provides further evidence about the initial PTFE morphology, because polymers with relatively large crystalline fractions generally exhibit small diffusion rates due to impermeability of the crystals. Thus, it is surprising that the unstrained PTFE exhibits a diffusion rate approximately equal to the specimen strained to 50%, when the morphological changes, which occur during elongation, are expected to increase the permeability of the semicrystalline films. However, one can visualize the film as containing crystalline zones connected by the polymer chains that pass through the amorphous phase of the film. It is known that the permeability of semicrystalline films is dependent upon the number of such 'tie molecules' which are pulled taut[6] and hinder the movement of other amorphous-phase chains. Our data indicate that, for PTFE in its original state, the tie molecules are in a relaxed state and do little to hinder the diffusion through the amorphous regions. This is not surprising, because the glass transition temperature ($T_g$) of PTFE is approximately 50°C, which allows sufficient freedom of molecular movement at room temperature to relieve most of the stresses within the network.

Finally, one could conceivably argue that the transitions detected in the diffusion experiment, conducted as a function of strain, are related to the entropic and enthalpic effects in the network[25] and do not necessarily result from the rotation of crystallites. In an attempt to show that energy changes are involved in this phenomenon, it should be realized that the diffusion through a polymer network requires energy and typically involves multiple steps: movement of polymeric chains in an effort to form a diffusion site for permeant molecule, or free volume distribution changes, followed by breaking interactions with surrounding polymer segments and actual diffusion. While the first step is primarily entropy driven, the remaining steps depend upon the mobility of diffusant molecules or network compatibility, and are thus of enthalpic origin. These, in turn, will be affected by the number and strength of interactions between the polymer network sites and diffusant molecules, factors that will inherently decide the overall enthalpy of diffusion. Since these types of interactions are usually of a short range, enthalpy is highly dependent upon the efficiency of polymer packing around the diffusant molecule, and therefore amorphous phase density.

In an effort to correlate morphological changes that occur in PTFE as a result of uniaxial elongations with

the enthalpy and entropy changes, *Figure 7* was constructed. For 0–4% strains (*Figure 7a*), diffusion decreases because tightening of tie molecules results in reduced freedom of motion in amorphous regions. Entropy most likely decreases, as the amorphous regions become more ordered. For strains ranging from 4 to 12% (*Figure 7b*), crystallites perpendicular to the film plane rotate. As a result, diffusion increases due to the larger free volume increases, giving more diffusion sites which, in turn, result in fewer diffusant–polymer interactions, leading to increased entropy and decreased enthalpy. As indicated in *Figure 6*, for strains of 12 to 18%, diffusion decreases again because crystallites rotate to a parallel position (*Figure 7c*), and due to a limited number of available diffusion sites giving entropy decrease, more diffusant–polymer interactions, resulting in enthalpy increase, are anticipated. Finally, for strains ranging from 18 to 50%, void formation, chain rupture and crystal slippage (*Figure 7d*) enhance diffusion (*Figure 6*), and enthalpic and entropic considerations are no longer valid as permanent voids are created.

## CONCLUSIONS

This study demonstrates that PTFE exhibits an *NPR* which is attributed to the rotation of crystals perpendicular to the draw direction. R.p.a. *FT*i.r. experiments allow direct measurement of permeability as a function of strain, which in turn can provide further insights into the submicroscopic morphological changes occurring during polymer elongation. X-ray diffraction, in combination with the r.p.a. *FT*i.r. method, enabled the formulation of a plausible mechanism for the occurrence of an *NPR* in PTFE. In spite of our efforts, transmission *FT*i.r. strain dichroism measurements conducted on PTFE do not show the *NPR* transition, substantiating our previous findings that photoacoustics may be a useful approach in examining stress–strain response in polymers.

## ACKNOWLEDGEMENTS

The authors are grateful to NRECA (Washington, DC, USA) for partial financial support of this study.

## REFERENCES

1 Peterlin, A. *J. Macromol. Sci.* 1975, **B11**, 57
2 Meares, P. *Eur. Polym. J.* 1966, **2**, 95
3 Phillips, J. C. and Peterlin, A. *Polym. Eng. Sci.* 1983, **23**, 734
4 Williams, J. L. and Peterlin, A. *J. Polym. Sci., Part A-2* 1971, **9**, 1483
5 Michaels, A. S. and Bixler, H. J. *J. Polym. Sci., Polym. Phys. Edn* 1961, **50**, 413
6 Vittoria, V., DeCandia, F., Capodanno, V. and Peterlin, A. *J. Polym. Sci., Polym. Phys. Edn* 1986, **24**, 1009
7 Ludwig, B. W. and Urban, M. W. *Polymer* 1992, **33**, 3343
8 Yasuda, H., Stannet, V., Frisch, H. L. and Peterlin, A. *Makromol. Chem.* 1964, **73**, 188
9 Heffelfinger, C. J. *Polym. Eng. Sci.* 1978, **18**, 1163
10 Caddock, B. D. and Evans, K. E. *J. Phys. D: Appl. Phys.* 1989, **22**, 1877
11 Evans, K. E. and Caddock, B. D. *J. Phys. D: Appl. Phys.* 1989, **22**, 1883
12 Ludwig, B. W. and Urban, M. W. *Polymer* 1993, **34**, 3376
13 Huong, J. B. and Urban, M. W. *J. Chem. Phys.* 1993, **98**(7), 5259
14 Starkweather, H. W. *Macromolecules* 1977, **10**, 1161
15 McDonald, W. F., Goettler, H. and Urban, M. W. *Appl. Spectrosc.* 1989, **43**, 1387
16 McDonald, W. F. and Urban, M. W. *J. Adhes. Sci. Technol.* 1990, **9**, 751
17 Urban, M. W. *Adv. Chem. Ser.* 1993, **236**, Ch. 21, p. 645
18 Brandrup, J. and Immergut, E. H. (Eds) 'Polymer Handbook', Wiley Interscience, New York, 1989
19 Thompson, H. W. and Temple, R. B. *Trans. Faraday Soc.* 1945, **41**, 236
20 Vergnound, J. M. 'Liquid Transport Properties in Polymeric Materials: Modeling and Industrial Applications', Prentice Hall, Englewood Cliffs, 1991
21 Crank, J. 'Mathematics of Diffusion', Oxford University Press, Oxford, 1957
22 Wecker, S. M. PhD Thesis, Northwestern University, Evanston, IL, USA, 1973
23 Meares, P. *J. Polym. Sci.* 1958, **26**, 391
24 Ng, H. C., Leung, W. P. and Choy, C. L. *J. Polym. Sci., Polym. Phys. Edn* 1985, **23**, 973
25 Flory, P. S. 'Principles of Polymer Chemistry', 13th edn, Cornell University Press, Ithaca, 1986